# 3D puzzle reconstruction for archeological fragments

F. Jampy*, A. Hostein**, E. Fauvet*, O. Laligant*, F. Truchetet*
*Le2i, UMR 6306 CNRS-Université de Bourgogne, **AnHiMA, UMR 8210 CNRS-Université Paris 1

## ABSTRACT

The reconstruction of broken artifacts is a common task in archeology domain; it can be supported now by 3D data acquisition device and computer processing. Many works have been dedicated in the past to reconstructing 2D puzzles but very few propose a true 3D approach. We present here a complete solution including a dedicated transportable 3D acquisition set-up and a virtual tool with a graphic interface allowing the archeologists to manipulate the fragments and to, interactively, reconstruct the puzzle. The whole lateral part is acquired by rotating the fragment around an axis chosen within a light sheet thanks to a step-motor synchronized with the camera frame clock. Another camera provides a top view of the fragment under scanning. A scanning accuracy of $100\mu m$ is attained. The iterative automatic processing algorithm is based on segmentation into facets of the lateral part of the fragments followed by a 3D matching providing the user with a ranked short list of possible assemblies. The device has been applied to the reconstruction of a set of 1200 fragments from broken tablets supporting a Latin inscription dating from the first century AD.

**Keywords:** 3D acquisition, 3D reconstruction, puzzle, archeology

## 1. INTRODUCTION

The reconstruction of broken artifacts is a common task in archeology domain. This activity is not the rewarding part of the archeologist work but one of the more time consuming and it can be supported now by 3D data acquisition device and computer processing. Those new technics are very useful in this domain for they allow to handle remotely very accurate models of fragile parts, they permit to test extensively reconstruction solutions and they provide access to the parts to the whole researcher community.

A large state of the art about both 3D scanning of archeological parts and broken artifact reconstruction can be found in the following references[1,2,3,4,5,6,7,8,9,10] Through those references it appears that true 3D approach for puzzle reconstructing is still an open problem for which the dimensional curse is to be broken.

An interesting problem has been recently proposed by archeologists under the form of a huge puzzle composed of a thousand of fragments of pentelic marble of different sizes found in Autun France, all attempts to reconstruct the puzzle during the last two centuries have failed. Those fragments seem to be parts of Latin inscription dating from the first century AD. They come from large marble tablets and their individual size ranges from few to 20 centimeters. Archeologists are sure that some fragments are missing and that some of the ones we have come from different tablets.[11]

The archeologist asks for a virtual tool to manipulate 3D representations of the fragments, suggest matching possibilities and simulate the reassembly of the fragments.

A first solution dealing with a known assembly of some fragments is proposed here: it starts from the acquisition of a fragment to the 3D reassembly of several fragments with an estimate of its likelihood.

The conclusion will presents some perspectives for completing our prototype in order to solve this challenging complex 3D puzzle reconstruction.

frederic.truchetet@u-bourgogne.fr

Figure 1. 3D acquisition set-up

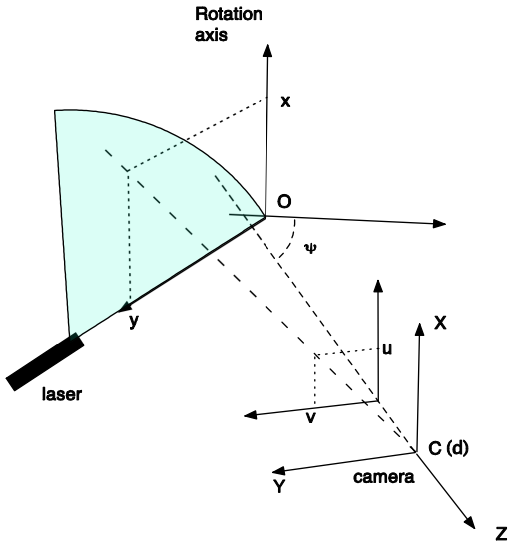


Figure 2. Set-up description

## 2. ACQUISITION SET-UP

### 2.1 Description

The acquisition system must follow some guide lines; we need to have a low cost transportable device, the system must also be usable by a museum for later acquisition of fragments. In order to optimized both performance and cost, a special dedicated set up has been designed. As the most important part of the pieces for puzzle reconstruction is the lateral one, we choose to get a 3D view of it with a line scanner based on a simple triangulation principle using a camera and a laser light sheet as illustrated on the figure 1. The whole lateral part is acquired by rotating the fragment around an axis chosen within the light sheet thanks to a step-motor synchronized with the camera frame clock. Another camera provides a top view of the fragment under scanning. A geometrical representation of this set-up is shown on figure 2. If $\alpha$ and $\beta$ are the intrinsic camera parameters,

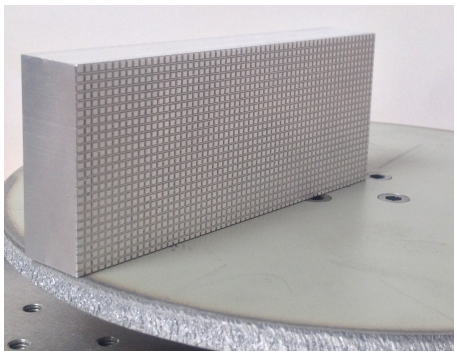

Figure 3. Calibration piece

$\psi$, $t_1, t_2, t_3$, the extrinsic ones, the transformation matrix is given by

$$\begin{aligned} A[Rt] &= \begin{bmatrix} \alpha & 0 & 0 & 0 \\ 0 & \beta & 0 & 0 \\ 0 & 0 & 1 & 0 \end{bmatrix} \begin{bmatrix} 1 & 0 & 0 & t_1 \\ 0 & \cos\psi & \sin\psi & t_2 \\ 0 & -\sin\psi & \cos\psi & t_3 \\ 0 & 0 & 0 & 1 \end{bmatrix} \\ &= \begin{bmatrix} \alpha & 0 & 0 & \alpha t_1 \\ 0 & \beta\cos\psi & \beta\sin\psi & \beta t_2 \\ 0 & -\sin\psi & \cos\psi & t_3 \end{bmatrix} \end{aligned} \tag{1}$$

and the coordinates of the image of a 3D point, denoted by $(u, v)$ are given by

$$\begin{bmatrix} su \\ sv \\ s \end{bmatrix} = \begin{bmatrix} \alpha & 0 & 0 & \alpha t_1 \\ 0 & \beta\cos\psi & \beta\sin\psi & \beta t_2 \\ 0 & -\sin\psi & \cos\psi & t_3 \end{bmatrix} \begin{bmatrix} x \\ y \\ z \\ 1 \end{bmatrix} \tag{2}$$

As $z = 0$, after resolving the system:

$$\begin{aligned} x &= \frac{u}{\alpha}\left(\frac{\beta t_2 + t_3\beta\cot\psi}{\beta\cot\psi + v}\right) - t_1 \\ y &= \frac{vt_3 - \beta t_2}{\beta\cos\psi + v\sin\psi} \end{aligned} \tag{3}$$

The six independent parameters are measured during the calibration stage.

### 2.2 Calibration[12,13]

The calibration process is made easy and efficient by a special disposition: the fragment rotation axis is chosen in the light sheet and parallel to the sensor plane and to the vertical axis of the sensor. Therefore the number of parameters to be determined is reduced to 5 (instead of 11 in the general case)[14] The calibration can be therefore done with only two characteristic points whose 3D coordinates are known. In fact, to achieve an optimal resolution we use a calibration piece with an engraved grid (see figure 3) set on the rotating stage in a known position. A simple line detection algorithm followed by a linear regression allows to obtain a precision better than the resolution provided by the camera.

### 2.3 Experiments and accuracy

The precision and resolution depend on the camera resolution, on the calibration and on the distance between the point under consideration and the rotation axis ( therefore its position on the image). With our 800x1200 pixels camera and the calibration process described in the previous section we have measured a precision better than

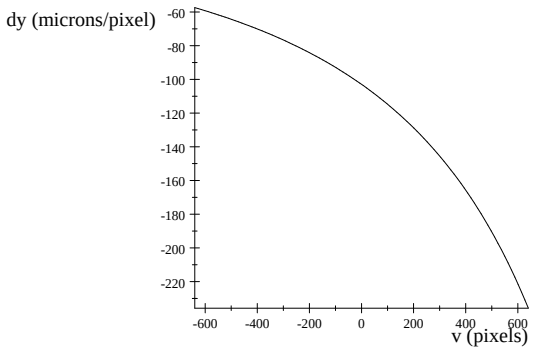


Figure 4. Example of dependency of the precision with respect to the distance to the axis of rotation

$100\mu m$ for the most remote points. An example of the dependency of this precision versus horizontal coordinate is given in figure 4.

Another important property is the visibility of a given point of the fragment (see illustration on figure 5). We have developed a method aiming at finding the best position of the object on the rotation stage (rotation axis position: K) for the largest visibility range and the best resolution. The bottom view is used for that in a preliminary step of the acquisition process. The system gives an information about the eventually missing points and the minimum theoretical resolution.We denote by $\Omega_K$ the region on which all possible rotation axes $K$ can

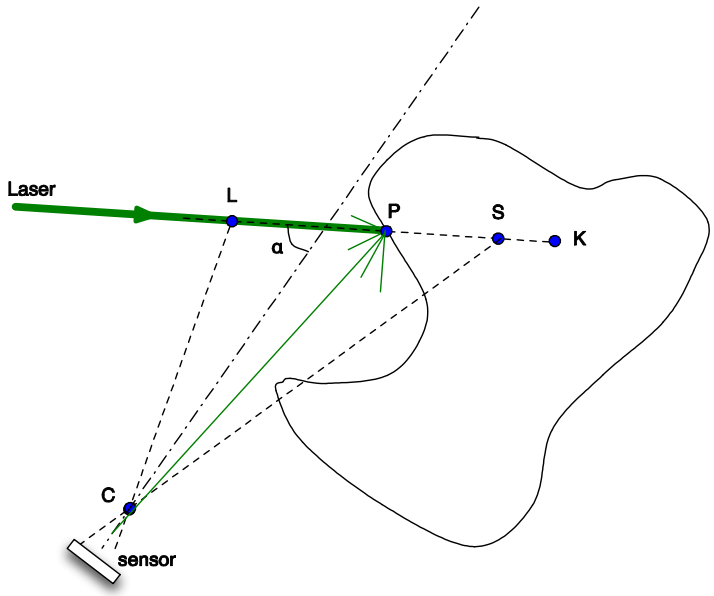


Figure 5. Visibility of a point P depending on the rotation center K

be chosen, $\omega_P$ denotes the known set of (seen from the bottom view) image points of the contour. For every $K \in \Omega_K$, we must verify that $P \in [LS]$. We have defined two criteria for characterized the result::

- visibility of $P_n$:

$$\nu(P_n) = \frac{\text{Card}(\Omega_{K/P_n})}{\text{Card}(\Omega_K)} \tag{4}$$

with $\Omega_{K/P_n}$ the set of $K$ allowing $P_n$ to be visible

- optimality of $K_l$ :

$$\lambda(K_l) = \frac{\text{Card}(\omega_{P/K_l})}{\text{Card}(\omega_P)} \tag{5}$$

  with $\omega_{P/K}$ the set of $P$ visible with $K_l$ as rotation center

The algorithm is given below:

- for every $K \in \Omega_K$
  - for every rotation step
    - verify that $P \in [LS]$
    - verify that $P$ is not hidden by an occultation
    - store $K$ corresponding to $P$
  - store the number of visible $P$
- build the visibility map $\nu$ (scores of visible $P$)
- build the optimality map $\lambda$ ( scores of $K$ giving the best visibility)

An example of visibility and optimality maps is given in figures 6 and 7.

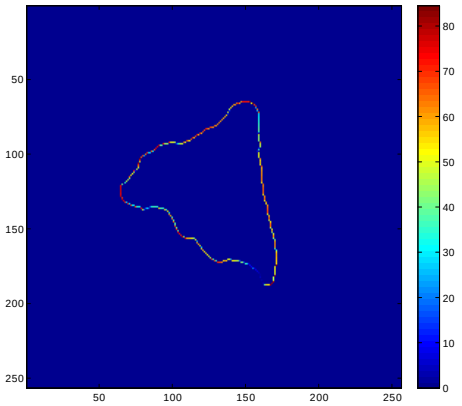


Figure 6. Visibility map

The optimality rarely goes beyond 70%. Consequently a first acquisition is achieved with the center leading to the best optimality. Then, a second pass is done by choosing a center computed from the remaining non-visible points.

The acquisition time depends on the angular resolution of the rotation. For a 1° unit step, the acquisition time for one fragment is about 1mn. In order to obtain a constant resolution we modulate the angular step with respect to the mean distance between the slice under scanning and the rotation axis. This distance is assumed to be approximately proportional to the line image mean ordinate: $\langle v \rangle$.

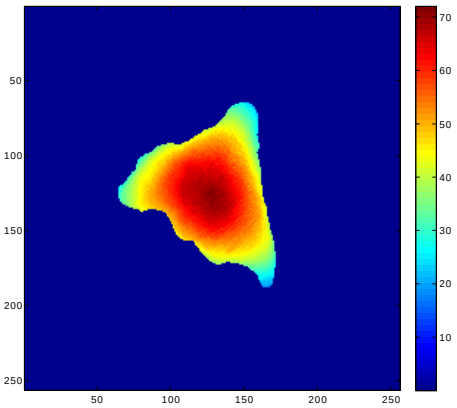


Figure 7. Optimality map

Figure 8. Example of raw 3D point cloud

## 3. PROCESSING

The processing is be divided into 3 stages:

- data preprocessing: data cropping and denoising
- facet segmentation
- facet matching and fragments merging

For every rotation angle, the projection of the laser line on the fragment is seen by the camera, an edge detection algorithm allows to extract the image of the line and, according to calibration, the 3D position of each point of the line is computed and after a complete rotation a raw 3D point cloud is get (see an example in figure 8) after automatic denoising based on thresholding set according to the neighboring density, a cloud of points ready to be processed is stored (figure 9).,

The most sensitive step is the segmentation. The elementary problem is to find two adjacent fragments. To limit the computational time and as we know that two adjacent fragments share at least one fractured facet and in the majority of cases, only one, we propose to segment the cloud of points representing the lateral part of a given fragment into facets in order to reduce the number of points used for each matching trial. An iterative segmentation algorithm, in which Ransac plane fitting is used as initialization step,[15] has been implemented to segment the fragment model into facets. At each iteration, each point is affected to the nearest plane, if the distance from the nearest plane is above a threshold belonging to the object geometry; a new plane is created in order to regroup all the points without facet affectation. Facets are merged or split according to the normal dissimilarity of the fitted plane, the proximity of points and the continuity of the facets. The main advantage

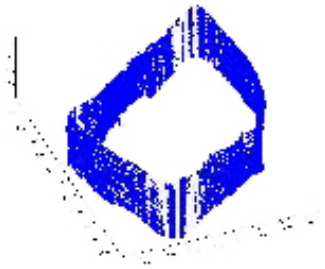

Figure 9. 3D point cloud after denoising

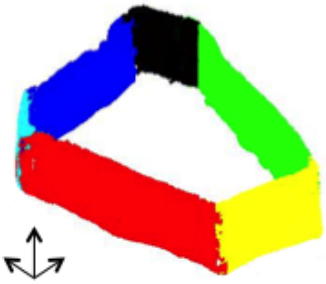

Figure 10. Fragment lateral part segmented into facets

is that no pre-knowledge of the fragment is required. An example of facet segmented fragment is shown in figure 10. The matching problem is similar to the registration one, therefore a slightly modified version of an Iterative Closest Points (ICP) algorithm[16,17] has been used. The residual error of the ICP gives us a likelihood estimate for the matching. Once the matching is validated by the archeologist, the two fragments are merged and considered after that as only one. The process of facet segmentation is performed again and a matching with the remaining fragments can be tried. The process can be iteratively repeated as far as fragments stay alone.

## 4. RESULTS

A graphic interface has been developed allowing the archeologist to supervise the process of fragment matching and merging. The first fragment is selected by the expert and the automatic process proposes few ranked solutions for matching pieces. After expert validation the iterative process can run up to the next matching proposition.

An example of digitized set of fragments is shown here as an illustration of the current state of our work. In this example 3 iterations has been done leading to the automatic reconstruction of the set shown in figures 11 and 12. These results has been obtained by selecting automatically the first ranked result for each pairwise matching.

## 5. CONCLUSION AND FUTURE WORKS

We have developed a complete solution for the acquisition and reconstruction of fragmented 3D objects figuring

- a transportable acquisition system providing 3D scans of the object contours and 2D images of their faces,
- a reconstruction method based on the congruence of two adjacent fragments.

This flexible solution is adapted to any similar problem of broken artifact with arbitrary shape, as fresco, murals, tablets or even in medicine[18] for orthopedists aiming at reconstructing heavily broken bones.

The next step, currently under progress, is to digitize the whole number fragments with the 2D/3D image of the carved face and also the 3D acquisition of the lateral face.

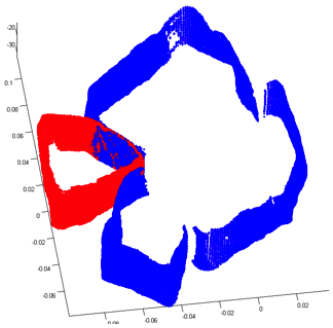

Figure 11. Automatic assembly of matching fragments

Figure 12. Example of reconstructed part

Some evolutions of the process are planned such as adding the optical character recognition from the image of the carved face. We also target some time consuming task of the process. Contour extraction is one of them, the sharp edge detection were not used here, discard due to a lot of smooth transition between the face but can give interesting result in combination with the actual iterative method. The matching part of the process is another option due to the number of use during the process. In,[19] Huang et al. propose a modification of the ICP algorithm which can solve the problem of collision between two fragments, adapted to our problem it will probably give a better adjustments of correct matching and reduce the number of false positive by increasing the residual errors in this cases.

The last evolution of the prototype will concern the integration of additional data from geologists, archeologists and historians to finally obtain a tool helping the reconstruction of this very challenging puzzle reconstruction.

## ACKNOWLEDGMENTS

We want to thanks Musée Rollin, Autun, for allowing us to scan the fragments.

This work has been done with the support of a CNRS grant, PEPS HuMaIn 2013&14 and LABEX HASTEC 2014.

## REFERENCES

1. D. Leitao, H. Solfi, and J. Solfi, "Automatic reassembly of irregular fragments," Tech. Rep. IC-98-06, Univ. of Campinas, 1998.
2. H. G. Leitao and J. Stolfi, "Information contents of fracture lines," in *proc. of WSCG'2000*, **2**, pp. 389–395, 2000.
3. H. G. Leitao and J. Stolfi, "A multiscale methof for the reassembly of two-dimension fragmented objects," *IEEE Trans. on PAMI* **24**(9), pp. 1239–1251, 2002.

4. W. Kong and B. Kimia, "On solving 2d and 3d puzzles using curve matching," in *Computer Vision and Pattern Recognition*, I. C. Society, ed., 2001.
5. S. Winkelbach and F. M. Wahl, "Pairwise matching of 3d fragments using cluster trees," *Int. J. Comput. Vis.* (78), pp. 1–13, 2008.
6. J. C. McBride and B. B. . Kimia, "Archaeological fragments reconstruction using curve-matching," in *Proc. of Computer Vision and Pattern Recognition Workshop*, IEEE, ed., 2003.
7. G. Papaioannou, E. Karabassi, and T. Theoharis, "Reconstruction of three-dimensional objects through matching of their parts," *IEEE Trans. on PAMI* **24**(1), pp. 114–124, 2002.
8. G. Papaioannou and E. Karabassi, "On the automatic assemblage of arbitrary broken solid artefact," *Image and Vision Computing* **21**, pp. 401–412, 2003.
9. Q. H. Y. L. Y. H. Pottmann, J. Wallner, "Integral invariants for robust geometry processing," Tech. Rep. 146, Geometry Preprint Series, Vienna U. of Tech., 2005.
10. N. Mellado, P. Reuter, and C. Schlick, "Semi-automatic geometry-driven reassembly of fractured archeological objects," in *proc. of the 11th Int. Symp. on Virtual Reality, Archaeology and Cultural Heritage VAST*, 2010.
11. E. Fauvet, A. Hostein, F. Jampy, O. Laligant, and F. Truchetet, "Digital epigraphy," in *JAAAB 2014*, 2014.
12. O. Faugeras, *Three dimensional computer vision: a geometric viewpoint*, MIT Press, 1993.
13. C. Chen and E. Kak, "Modeling and calibration of a structured light scanner for 3d robot vision," in *Proc. of IEEE conf. on Robotics and Automation*, IEEE, ed., pp. 807–815, 1987.
14. J. Forest, J. Calvi, E. Cabruja, and M. Bigas, "Projective calibration of a laser 3d scanner using the complete quadrangle." 2003.
15. M. Fischler and R. Bolles, "Random sample consensus: a paradigm fro model fitting with applications to image analysis and automated cartography," *Communications of the ACM* **24**(6), pp. 381–395, 1981.
16. P. Besl and N. McKay, "A method for registration of 3-d shapes," *IEEE Trans. on PAMI* **14**(2), pp. 239–255, 1992.
17. Y. Chen and G. Medioni, "Object modelling by registration of multiple range images," *Image and vision computing* **10**(3), pp. 145–155, 1992.
18. T. Thomas, D. Anderson, A. Willis, P. Liu, M. Frank, J. Marsh, and T. Brown, "A computational/experimental platform for investigating three-dimensional puzzle solving of comminuted articular fractures," *Comput. Methods Biomed. Engin.* **14**(3), pp. 263–270, 2011.
19. Q.-X. H. andS. Flöry, N. Gelfand, M. Hofer, and H. Pottmann, "Reassembling fractured objects by geometric matching," *ACM Transactions on Graphics* **25**(3), pp. 569–578, 2006.